Journal of Southeast University (English Edition) Vol. 41, No. 1, pp. 27-36 Mar. 2025 ISSN 1003-7985

Influence study of main cable displacement-controlled device type of long-span suspension bridges on structural mechanical properties

YUAN Zhijie[1,2], WANG Hao[1], MAO Jianxiao[1], LI Rou[1], ZONG Hai[3]

(1. Key Laboratory of Concrete and Prestressed Concrete Structures of Ministry of Education, Southeast University, Nanjing 211189, China; 2. Laboratorio di Meccanica della Frattura, Politecnico di Torino, Torino 10129, Italy; 3. Nanjing Highway Development (Group) Co., Ltd., Nanjing 210031, China)

Abstract: Main cable displacement-controlled devices (DCDs) are key components for coordinating the vertical deformation of the main cable and main girder in the side span of continuous suspension bridges. To reveal the mechanical action mechanisms of DCD on bridge structures, a three-span continuous suspension bridge was taken as the engineering background in this study. The influence of different forms of DCD on the internal force and displacement of the components in the side span of the bridge and the structural dynamic characteristics were explored through numerical simulations. The results showed that the lack of DCD caused the main cable and main girder to have large vertical displacements. The stresses of other components were redistributed, and the safety factor of the suspenders at the side span was greatly reduced. The setting of DCD improved the vertical stiffness of the structure. The rigid DCD had larger internal forces, but its control effect on the internal forces at the side span was slightly better than that of the flexible DCD. Both forms of DCD effectively coordinated the deformation of the main cable and main girder and the stress distribution of components in the side span area. The choice of DCD form depends on the topographic factors of bridge sites and the design requirements of related components at the side span.

Key words: long-span suspension bridge; displacement-controlled device; static and dynamic characteristics; finite element; live load

DOI: 10.3969/j.issn.1003-7985.2025.01.004

With the advancement of major national strategic plans, China's demand for modern transportation infrastructure construction is becoming increasingly urgent[1-3]. Because of their reasonable structural force systems and strong spanning capacities, long-span suspension bridges have become the popular choice for large crossing scenes, such as wide rivers and valleys[4-8]. Among them, continuous suspension bridges have the advantages of high stiffness, good comprehensive wind resistance and stability, and high driving comfort[9] and have been widely used in recent years[10-15].

During the structural design phase, a relevant study[16] found that because of the continuity of the main girder and the constraints of terrain conditions, the side span of the main girder of continuous system suspension bridges often cannot cover the main cable area of the side span. The linear shape of the main girder and main cable is difficult to effectively guarantee under the action of gravity and vehicle loads. To adapt to the overall layout of a structure, Qi et al.[17] and Wang et al.[18-19] proposed the use of a main cable flexible displacement-controlled device (DCD) and a main cable rigid DCD to control the alignment of the main cable and main girder in the side span area.

In engineering, flexible DCD must be anchored on bridge piers through steel strands to form a series system. The entire system is finally anchored on the foundation, which is called the displacement-controlled suspender (DCS) system. Meanwhile, rigid DCD is usually a steel-concrete structure tower. Both types of DCDs can effectively control the alignment of the main cable and main girder of the side span and coordinate their vertical deformation relationships. The choice of DCD form is related to the topographic factors of the bridge site.

To ensure the service performance of continuous suspension bridge structures and analyze the mechanical action mechanism of DCD, the influence of different forms of DCD on the static and dynamic characteristics of a structure must be studied. Although DCD has been applied in suspension bridges, there have been only a few studies on the mechanical analysis of different types of DCDs under different loading conditions. For instance, Yuan et al.[20] and Wu[21] studied the influence of flexible DCD on the static and dynamic characteris-

Received 2024-08-08, **Revised** 2024-11-25.

Biographies: Yuan Zhijie (1995—), male, Ph. D. candidate; Wang Hao (corresponding author), male, doctor, professor, wanghao1980@seu.edu.cn.

Foundation items: The National Natural Science Foundation of China (No. 52338011), the Postgraduate Research & Practice Innovation Program of Jiangsu Province (No. SJCX23_0067).

Citation: YUAN Zhijie, WANG Hao, MAO Jianxiao, et al. Influence study of main cable displacement-controlled device type of long-span suspension bridges on structural mechanical properties[J]. Journal of Southeast University (English Edition), 2025, 41(1): 27-36. DOI: 10.3969/j.issn.1003-7985.2025.01.004.

tics of continuous suspension bridges. Regrettably, no reports on the research of rigid DCD were found despite its crucial role in the structural analysis of long-span bridges.

This paper further establishes the comparative analysis models based on the research of Yuan et al. [20]. The influence of different DCDs on the main cable line shape, main girder line shape, internal force, and dynamic characteristics of key components are deeply analyzed through numerical simulations. The mechanical mechanism of DCD's effect on a structure was analyzed, and the rationality of DCD was explained from a physical mechanism perspective. The research results can provide the necessary information and research basis for the health monitoring of bridges and can provide a reference for the design and application of DCDs in continuous system suspension bridges in the future.

1 Engineering Background and Finite Element Model

The span arrangement of the studied three-span continuous suspension bridge is 576.2 m + 1 418 m + 481.8 m. The main girder is a continuous steel box girder with a total width of 38.8 m and a girder height of 3.5 m. The main cable span ratio is 1/9, and the sag is 157.5 m. The main cable adopts 127ϕ5.35 mm prefabricated parallel steel wire strands with a tensile strength of 1 770 MPa. The suspenders are composed of prefabricated parallel steel wire strands with a tensile strength of 1 670 MPa, arranged at intervals of 15.6 m. A steel-concrete structure is used in the construction of the cable tower, which is 227.2 m high. The overall structure is shown in Fig. 1.

Fig. 1 Engineering background

As mentioned in the introduction, at the outermost side of the side span, flexible DCD is applied. The DCD is essentially a DCS consisting of 295 steel wires. The upper end of the DCS is connected to the cable clamp, and the bottom is anchored in the anchor box inside the top of the transition pier by 12 MJ80 anchor rods. The whole structure is finally anchored to the foundation, as shown in Fig. 2.

According to the design data and construction drawings, a three-dimensional finite element (FE) model of

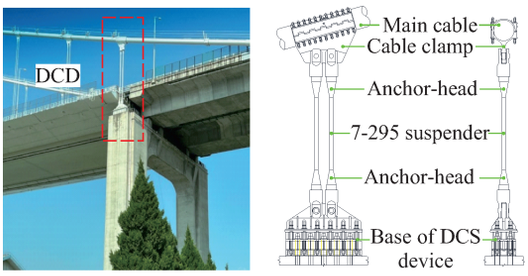

Fig. 2 Displacement-controlled suspender. (a) Overall appearance; (b) Detailed structure

the structure was established using ANSYS, as shown in Fig. 3. LINK10 element was used to simulate the main cable and suspender system (including the flexible DCD). BEAM4 element was used to simulate the main girder and the tower. The initial stress of the main cable was considered in the form of element initial strain[22]. Spring-damper elements (i.e., Combin14 elements) were used to simulate the elastic supporting and longitudinal limiting effect between the pylons and girder, combining the behaviors of a spring and a damper. To consider the influence of geometric nonlinearity, the elastic modulus of the main cable was calculated using the Ernst equivalent elastic modulus formula[23].

According to the design data and modeling methods[24-25], the rotational freedom between the main girder and the main tower was coupled. All degrees of freedom of the main cable and the tower top were coupled. The bottom of the side cable and the DCD were treated as completely consolidated. The initial stresses of the structural components were adjusted so that the error between the structural line shape under the initial dead load and the completed bridge state was within the allowable range[26]. Then, stress stiffening was performed[27]. Previously, Yuan et al. [20] compared the measured data of static and dynamic characteristics with FE calculation results and proved the correctness of this model, so it is not repeated here.

On the basis of the bridge model with flexible DCD in Fig. 3, the element properties and section parameters of the flexible DCD in the model were modified into a rigid DCD; thus, a bridge model with rigid DCD was established. Notably, the rigid DCD was modeled using the BEAM4 element, and the selection of cross-sectional parameters was based on actual cases[18]. At the same time, a bridge model without DCD was also established to facilitate comparative analysis. In this paper, the model without DCD was named Model 1, the model with flexible DCD was named Model 2, and the model with rigid DCD was named Model 3. Using these three models, the influence of DCD on the static and dynamic characteristics of a structure was investigated in detail. Notably, Model 2 was the actual bridge state.

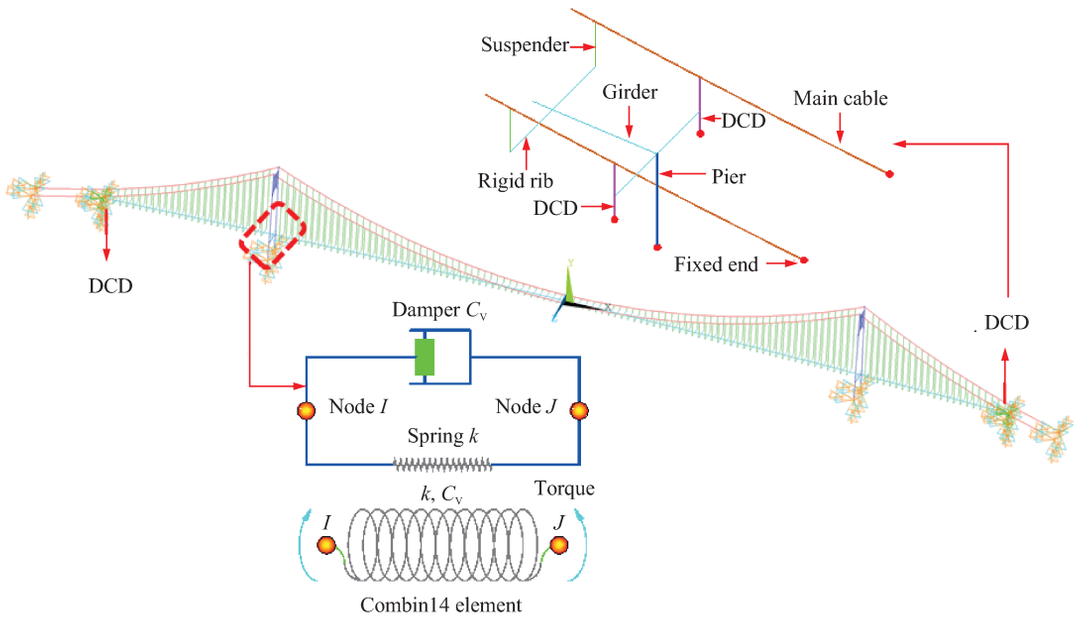

Fig. 3 Finite element model

2 Effect of DCD on Static Characteristics of Structure

To deeply analyze the influence of DCD on the static characteristics of a structure, dead load and uniformly distributed load conditions were calculated. The internal forces and displacements of key components were extracted for comparative analysis. According to the structural characteristics of the studied long-span suspension bridge, the selected evaluation indicators are shown in Table 1.

Table 1 Selection of calculation indicators

Internal force index	Displacement index
Internal force of the main girder mid-span	Mid-span deflection
Internal force of the main girder side span	Displacement of the girder end on the north side
Main cable internal force	Displacement of the girder end on the south side
Main tower internal force	Displacement of the main tower top
Axial force of DCD	Main cable line shape
Axial force of key suspenders	Main girder line shape

2.1 Dead load

Through numerical simulations, the internal force and displacement indices of the three models under dead load were calculated, as shown in Table 2. For Model 1, the side span of the main girder was subjected to a large internal force, which reached the maximum at the pier and gradually decreased along the longitudinal direction of the bridge. The linear shape of the main cable and main girder at the side span had a larger error compared with the completed bridge state. The internal forces of the main girder and side span were investigated, and the bending moment at the pier increased by 113.7 times compared with the completed bridge state, which significantly adversely affected the pier and the main girders. Although the axial force at the bottom of the main tower was not much different from that of the completed bridge, its bending moment increased by nearly two times. In addition, the absence of DCD led to a sharp increase in the suspender forces in the side span. The adjacent suspender at the DCD position was used as an example, and the safety factor of this suspender in the design state was as high as 3.9. When the DCD setting was canceled, the axial force of this sling increased by 3.3 times, causing its safety factor to drop to 1.2, which no longer met the safety requirements.

From the calculation of the displacement index, the displacement of the girder end did not change much because of the existence of the bridge pier. However, because of the lack of DCD, the linear shape of the main cables was greatly affected, and a large deflection occurred in the mid-span, which was seriously inconsistent with the state of the completed bridge. The top of the main tower experienced a large longitudinal displacement. The alignment of the main cables and main girders in Model 1 was investigated in depth, and the error between the alignment and the completed bridge state was calculated, as shown in Fig. 4.

As shown in Fig. 4, because of the lack of DCD, the main cable and main girder experienced large vertical deformations. When DCD was not set, the main cable of the side span underwent vertical upward displacement, and its displacement reached 355.3 mm. At this time,

Table 2 Calculation results under dead load

Calculation content		Specific location	Index	Model 1	Model 2	Model 3
Internal force index	Internal force of the mid-span	Main span midpoint	Axial force/kN	−12.91	−46.66	−46.60
			Bending moment/(kN·m)	4 612.53	4 921.09	4 921.49
	Internal force of the main girder on the north side span	Node at DCD	Axial force/kN	225.19	41.40	41.32
			Bending moment/(kN·m)	97 339.47	−856.20	−897.36
		Node of the suspender adjacent to DCD	Axial force/kN	10.66	34.02	34.04
			Bending moment/(kN·m)	69 633.33	−4 764.14	−4 795.19
		Midpoint of the side span	Axial force/kN	38.98	−16.56	−16.53
			Bending moment/(kN·m)	1 316.24	1 968.62	1 969.29
	Internal force of the north tower	Base of the main tower	Axial force/kN	−453 195.39	−453 559.55	−453 559.84
			Bending moment/(kN·m)	21 399.00	−10 848.00	−10 890.21
	Main cable internal force	Main cable midpoint	Axial force/kN	226 915.73	227 099.07	227 099.31
	Axial force of DCD	DCD on the north side	Axial force/kN		4 187.68	4 210.39
	Axial force of key suspenders	Suspender adjacent to DCD	Axial force/kN	5 921.56	1 787.58	1 785.85
		Short suspender at midpoint	Axial force/kN	1 720.63	1 720.62	1 720.62
Displacement index	Deflection	Midpoint	Displacement/mm	−95.61	0.27	0.27
	Displacement of the girder end	North side	Displacement/mm	−0.23	−0.28	−0.28
	Displacement of the girder end	South side	Displacement/mm	−0.25	−0.30	−0.30
	Displacement of the tower top	North side	Displacement/mm	−28.18	6.60	6.63

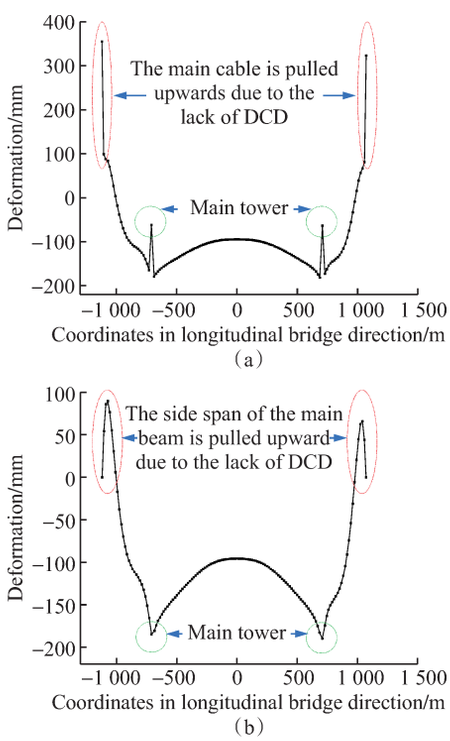

Fig. 4 Deformation of the main cable and main girder of Model 1 under gravity. (a) Main cable; (b) Main girder

the maximum positive deformation of the main girder was 89.5 mm, and the maximum negative deformation was −189.8 mm. In addition, because only the DCD was canceled, stress redistribution occurred in the suspender system, and the suspender tension in the side span increased sharply, causing this part of the main girder to deform upward because of the suspender tension. At the pier position, the suspender force gradually and smoothly transitioned to 0, and the main girder deformation reached the positive maximum value in this area. In the rest of the side span, the main girder deformed downward under the action of gravity, and the deformation direction changed at the main tower. The suspenders were tension-only members, so the main cables also displaced downward and changed direction at the main tower. The deformation laws of the main cable and main girder of the main span were consistent and distributed symmetrically.

The calculation results for Models 2 and 3 showed that under the action of gravity, there was no obvious difference in the influence of flexible DCD and rigid DCD on the static characteristics of the structure. Both models met the design status of the structure. Under deadweight conditions, the flexible DCD's own internal forces and its control over the internal forces of the side span components seemed to be slightly better than those of the rigid DCD.

2.2 Uniform load

According to the recommendations of the bridge load code, four groups of working conditions were set for the calculation to analyze the control effect of DCD on the main cable under uniformly distributed load, as shown in Table 3. The magnitude of the uniformly distributed load was set to 30 kN/m, and the direction was vertically downward.

The internal force and displacement indicators of the three models under four calculation cases were calculated

Table 3 Calculation cases

No.	Explanation
1	Only the mid-span is fully loaded
2	Only the two side spans are fully loaded
3	Only the middle span and the north side span are fully loaded
4	Only the middle span and the south side span are fully loaded

through numerical simulations. The specific results are shown in Tables 4 to 7. Apparently, the setting of DCD effectively controlled the internal force of the main girder and reduced the suspender force at the side span. The lack of DCD made the safety factor of the suspenders at the side span less than 1, and the structure faced greater safety hazards. In addition, the lack of DCD caused a large bending moment at the base of the main tower. Because of the absence of DCD, the deflection and displacement of the tower top in Model 1 were also the largest.

The comparative analysis showed that because of the

Table 4 Calculation results under Case 1

Calculation content		Specific location	Index	Model 1	Model 2	Model 3
Internal force index	Internal force of the mid-span	Main span midpoint	Axial force/kN	−115.93	−140.37	−52.10
			Bending moment/(kN·m)	218.96	680.87	999.07
	Internal force of the main girder on the north side span	Node at DCD	Axial force/kN	360.25	66.51	60.41
			Bending moment/(kN·m)	169 494.21	12 561.29	9 301.82
		Node of the suspender adjacent to DCD	Axial force/kN	−3.12	37.74	49.03
			Bending moment/(kN·m)	133 156.22	14 889.42	12 564.79
		Midpoint of the side span	Axial force/kN	149.7	72.57	126.98
			Bending moment/(kN·m)	27 272.21	28 211.85	28 627.16
	Internal force of the north tower	Base of the main tower	Axial force/kN	−471 583.30	−472 178.40	−472 335.97
			Bending moment/(kN·m)	286 668.13	237 389.18	205 289.71
	Main cable internal force	Main cable midpoint	Axial force/kN	247 738.45	248 035.36	248 244.42
	Axial force of DCD	DCD on the north side	Axial force/kN		6 738.27	11 986.06
	Axial force of key suspenders	Suspender adjacent to DCD	Axial force/kN	8 686.91	2 060.64	1 918.84
		Short suspender at midpoint	Axial force/kN	1 954.54	1 954.54	1 954.57
Displacement index	Deflection	Midpoint	Displacement/mm	−1 913.70	−1 730.54	−1 610.63
	Displacement of the girder end	North side	Displacement/mm	−0.19	−0.27	−0.27
	Displacement of the girder end	South side	Displacement/mm	−0.21	−0.29	−0.29
	Displacement of the tower top	North side	Displacement/mm	−306.31	−255.49	−223.23

Table 5 Calculation results under Case 2

Calculation content		Specific location	Index	Model 1	Model 2	Model 3
Internal force index	Internal force of the mid-span	Main span midpoint	Axial force/kN	−594.01	−607.03	−597.09
			Bending moment/(kN·m)	−11 514.92	−11 341.15	−11 314.80
	Internal force of the main girder on the north side span	Node at DCD	Axial force/kN	107.03	9.82	14.38
			Bending moment/(kN·m)	37 335.17	−14 601.94	−12 164.13
		Node of the suspender adjacent to DCD	Axial force/kN	−35.08	−6.14	−6.63
			Bending moment/(kN·m)	12 812.19	−26 513.32	−24 650.44
		Midpoint of the side span	Axial force/kN	−427.35	−447.01	−439.75
			Bending moment/(kN·m)	−27 364.01	−26 984.84	−26 951.48
	Internal force of the north tower	Base of the main tower	Axial force/kN	−458 119.10	−458 313.28	−458 328.06
			Bending moment/(kN·m)	−101 933.09	−118 788.34	−121 783.32
	Main cable internal force	Main cable midpoint	Axial force/kN	229 211.50	229 313.98	229 334.00
	Axial force of DCD	DCD on the north side	Axial force/kN		2 219.72	2 755.40
	Axial force of key suspenders	Suspender adjacent to DCD	Axial force/kN	3 986.88	1 790.35	1 892.19
		Short suspender at midpoint	Axial force /kN	1 852.02	1 852.04	1 852.09
Displacement index	Deflection	Midpoint	Displacement/mm	69.99	137.32	146.80
	Displacement of the girder end	North side	Displacement/mm	−0.26	−0.29	−0.29
	Displacement of the girder end	South side	Displacement/mm	−0.28	−0.31	−0.31
	Displacement of the tower top	North side	Displacement/mm	80.01	100.33	102.98

Table 6 Calculation results under Case 3

Calculation content		Specific location	Index	Model 1	Model 2	Model 3
Internal force index	Internal force of the mid-span	Main span midpoint	Axial force/kN	−384.92	−404.21	−309.21
			Bending moment/(kN·m)	875.80	1 253.12	1 575.51
	Internal force of the main girder on the north side span	Node at DCD	Axial force/kN	234.00	34.13	33.36
			Bending moment/(kN·m)	105 172.32	−1 612.07	−2 023.76
		Node of the suspender adjacent to DCD	Axial force/kN	−74.01	−5.28	5.64
			Bending moment/(kN·m)	73 331.66	−7 115.64	−7 277.80
		Midpoint of the side span	Axial force/kN	−331.87	−354.54	−291.32
			Bending moment/(kN·m)	−1 191.69	−464.92	−189.73
	Internal force of the north tower	Base of the main tower	Axial force/kN	−475 729.15	−475 839.01	−475 991.07
			Bending moment/(kN·m)	151 870.36	118 876.02	86 337.93
	Main cable internal force	Main cable midpoint	Axial force/kN	248 143.76	248 388.10	248 600.83
	Axial force of DCD	DCD on the north side	Axial force/kN		4 582.22	9 943.26
	Axial force of key suspenders	Suspender adjacent to DCD	Axial force/kN	6 551.12	2 040.98	2 018.92
		Short suspender at midpoint	Axial force/kN	1 954.48	1 954.48	1 954.51
Displacement index	Deflection	Midpoint	Displacement/mm	−1 639.29	−1 489.48	−1 368.09
	Displacement of the girder end	North side	Displacement/mm	−0.22	−0.28	−0.28
	Displacement of the girder end	South side	Displacement/mm	−0.21	−0.29	−0.29
	Displacement of the tower top	North side	Displacement/mm	−202.46	−257.72	−225.14

Table 7 Calculation results under Case 4

Calculation content		Specific location	Index	Model 1	Model 2	Model 3
Internal force index	Internal force of the mid-span	Main span midpoint	Axial force/kN	−402.67	−417.79	−319.78
			Bending moment/(kN·m)	−15 731.29	−15 310.79	−14 965.40
	Internal force of the main girder on the north side span	Node at DCD	Axial force/kN	368.18	67.95	61.48
			Bending moment/(kN·m)	173 735.42	13 331.94	9 872.00
		Node of the suspender adjacent to DCD	Axial force/kN	10.28	40.31	52.29
			Bending moment/(kN·m)	136 849.34	15 996.55	13 529.40
		Midpoint of the side span	Axial force/kN	183.04	89.73	148.05
			Bending moment/(kN·m)	28 714.24	29 643.83	30 084.13
	Internal force of the north tower	Base of the main tower	Axial force/kN	−472 642.08	−473 246.27	−473 424.26
			Bending moment/(kN·m)	305 442.98	154 922.10	200 484.11
	Main cable internal force	Main cable midpoint	Axial force/kN	249 616.37	249 881.81	250 109.42
	Axial force of DCD	DCD on the north side	Axial force/kN		6 902.89	12 536.90
	Axial force of key suspenders	Suspender adjacent to DCD	Axial force/kN	8 864.94	2 079.56	1 928.34
		Short suspender at midpoint	Axial force/kN	3 090.29	2 090.34	2 090.45
Displacement index	Deflection	Midpoint	Displacement/mm	−2 032.03	−1 869.38	−1 742.26
	Displacement of the girder end	North side	Displacement/mm	−0.19	−0.27	−0.27
	Displacement of the girder end	South side	Displacement/mm	−0.24	−0.30	−0.30
	Displacement of the tower top	North side	Displacement/mm	−202.46	−166.35	−131.98

different structures and force forms, the internal force of the rigid DCD was slightly greater than that of the flexible DCD. However, the overall control effect of the rigid DCD on the internal force of the side span main girder was slightly better than that of the flexible DCD. Both forms of DCD effectively coordinated the deformation and stress distribution of the main girder and main cable in the side span area.

The linear shapes of the main cable and main girder under various cases were investigated in depth, and the deformations of the main cable and main girder of the three models under four cases were calculated. The specific results are shown in Figs. 5 to 8. The control effect of DCD on the linear shape of the main cable and the main girder was very obvious in the four cases. When DCD was missing, the deformation of the main cable from the girder end to the pier was large, causing the main girder to move upward in this area. The deformation of the main girder and main cable gradually returned to 0 at the main tower and deformed downward at the mid-span,

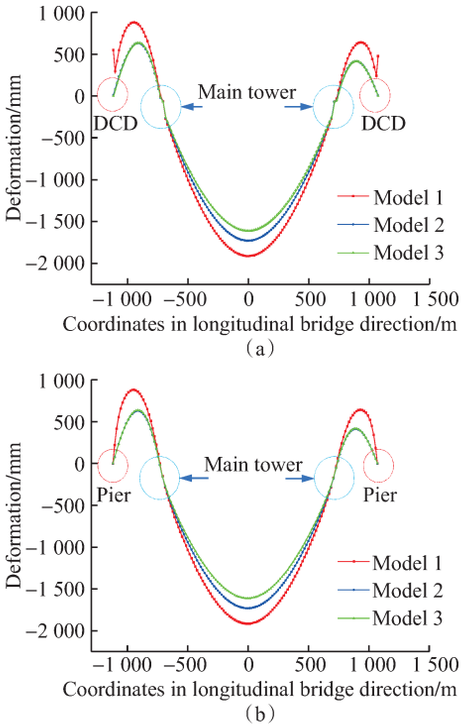

Fig. 5 Deformation under Case 1. (a) Main cable; (b) Main girder

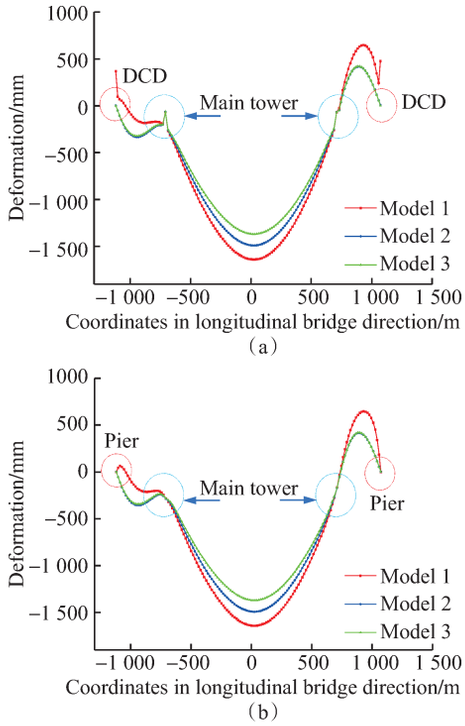

Fig. 7 Deformation under Case 3. (a) Main cable ; (b) Main girder

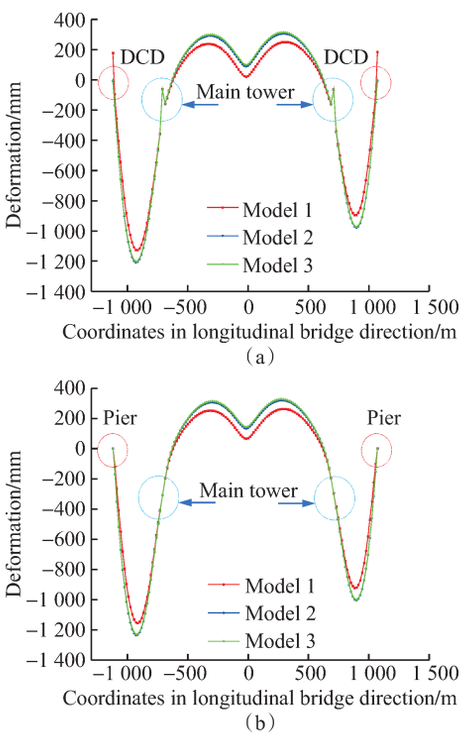

Fig. 6 Deformation under Case 2. (a) Main cable ; (b) Main girder

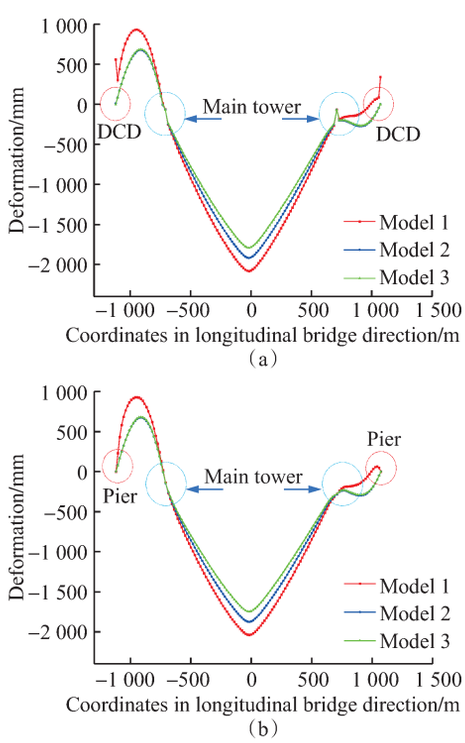

Fig. 8 Deformation under Case 4. (a) Main cable ; (b) Main girder

reaching the maximum value at the midpoint. Because of the presence of the bridge pier, the displacements of the end of the main girder in the three models were very small, but the deformation of Model 1 was significantly greater than that of the model containing DCD. On the whole, DCD not only can coordinate the deformation of the main cables and main girders in the side span area but also has a good control effect on deflection. In terms of the main cable and main girder line shape in the middle span, the control effect of rigid DCD is better than that of flexible DCD.

3 Effect of DCD on Dynamic Characteristics of Structure

To study the influence of DCD on the dynamic characteristics of the studied structure, the subspace iteration method[28-29] was used to analyze the dynamic characteristics of the three models. The first six vibration modes of the three models are shown in Fig. 9. The first 10 frequencies and vibration modes of the three models are listed in Table 8.

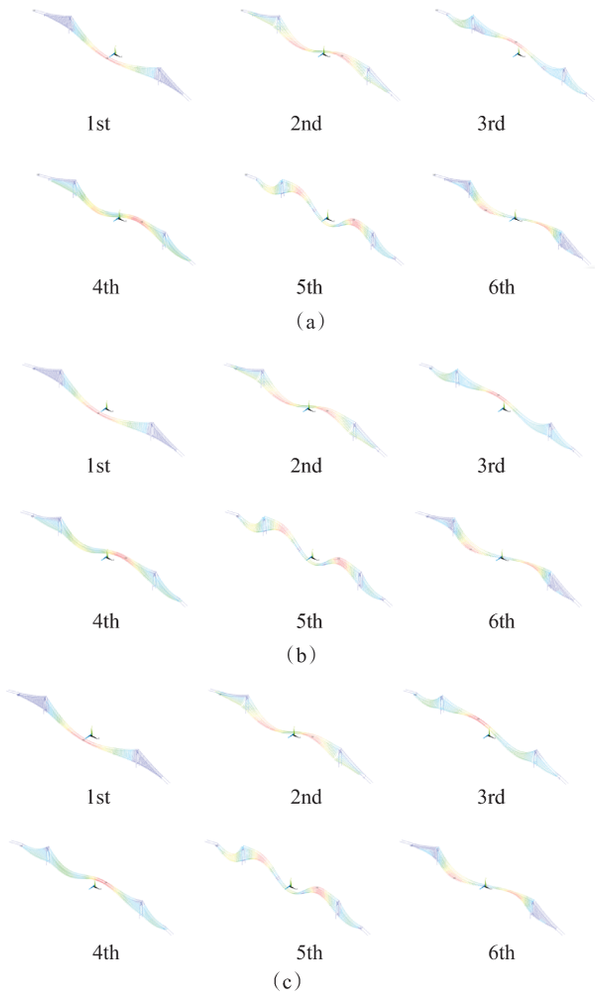

Fig. 9 First six vibration modes. (a) Model 1; (b) Model 2; (c) Model 3

The results of the FE analysis showed that the fundamental frequency of the bridge was about 0.063 Hz, with a relatively long fundamental period. The first corresponding vibration mode was the first-order symmetric lateral bending. The second-order vibration frequency of the bridge was about 0.078 Hz, and its corresponding vibration mode was the first-order antisymmetric vertical bending. The calculation results were consistent with the general laws of flexible structures of long-span suspension bridges[30]. Torsional vibration modes appeared in high-frequency vibrations, which were closely related to the vortex-induced vibration and flutter performance of the bridge. Flexible DCD had little impact on the dynamic characteristics of the bridge. Compared with Model 1, the frequencies of the first-order symmetric vertical bending, second-order symmetric vertical bending, third-order antisymmetric vertical bending, and third-order symmetric vertical bending vibration modes of Model 2 all increased, with the increase rates being 1.8%, 1.4%, 4.0%, and 1.4%, respectively. Because of the change in element structure, the frequencies of the rigid DCD models all increased. Combined with the results of static analysis, the existence of DCD apparently can improve the vertical stiffness of the continuous system suspension bridge.

Table 8 Dynamic characteristic analysis of the models

Frequency order	Frequency/Hz			Explanation
	Model 1	Model 2	Model 3	
1st	0.062 912	0.062 922	0.062 923	First lateral bending, symmetric
2nd	0.078 136	0.078 148	0.078 293	First vertical bending, antisymmetric
3rd	0.110 83	0.113 04	0.114 46	First vertical bending, symmetric
4th	0.115 77	0.116 23	0.116 54	Second vertical bending, antisymmetric
5th	0.144 23	0.146 18	0.146 68	Second vertical bending, symmetric
6th	0.152 64	0.152 65	0.152 67	First lateral bending, antisymmetric
7th	0.173 14	0.180 05	0.180 86	Third vertical bending, antisymmetric
8th	0.189 81	0.189 97	0.189 99	Second lateral bending, symmetric
9th	0.195 20	0.195 26	0.198 78	Second lateral bending, antisymmetric
10th	0.198 14	0.198 17	0.200 87	Fourth vertical bending, antisymmetric

4 Conclusions

(1) DCD significantly impacts the linear shape of the main cable and main girder of continuous suspension bridges. The lack of DCD causes large vertical displacements of the main cable and main girder at the side span and stress redistribution in the remaining suspenders, greatly reducing the safety factor of the suspenders at the side span.

(2) Flexible DCD mainly affects the first three vertical bending modal frequencies of continuous suspension bridges. The frequencies of structures containing rigid DCD are all increased.

(3) Because of its different types of structural elements, rigid DCD has larger internal forces, but its control effect on the internal forces of the main girder at the side span is slightly better than that of flexible DCD. Both forms of DCD can effectively coordinate the deformation and stress distribution of the main cable and main

girder in the side span area. The choice of DCD form depends on the topographic factors of the bridge site and the design requirements of the side span components.

References

[1] XUE J, ZHOU S J. Transportation and communication infrastructures: Development, regional disparities and economic effects [J]. Management Review, 2023, 35 (6): 3-14. (in Chinese)

[2] ZHANG X, WANG X, WAN G H, et al. A unified framework of road infrastructure's growth effect [J]. Economic Research Journal, 2018, 53 (1): 50-64. (in Chinese)

[3] BANERJEE A, DUFLO E, QIAN N. On the road: Access to transportation infrastructure and economic growth in China [J]. Journal of Development Economics, 2020, 145: 102442.

[4] NI Y C, ZHANG Q W, LIU J F. Dynamic performance investigation of a long-span suspension bridge using a Bayesian approach [J]. Mechanical Systems and Signal Processing, 2022, 168: 108700.

[5] RIZZO F, CARACOGLIA L, MONTELPARE S. Predicting the flutter speed of a pedestrian suspension bridge through examination of laboratory experimental errors [J]. Engineering Structures, 2018, 172: 589-613.

[6] WANG H, TAO T Y, ZHANG Y P, et al. Seismic control of long-span triple-tower suspension bridge under travelling wave action [J]. Journal of Southeast University (Natural Science Edition), 2017, 47(2): 343-349. (in Chinese)

[7] LUO L F, SHAN D S, CHEN F M, et al. High-precision calculation method for configuration of completed suspension bridges with pin-connected cable clamps [J]. Engineering Mechanics, 2021, 38 (8): 133-144. (in Chinese)

[8] LI Y L, QIAN Y Z, ZHU J, et al. Longitudinal vibration characteristics of a long-span highway suspension bridge under stochastic wind and traffic loads [J]. China Journal of Highway and Transport, 2021, 34 (4): 93-104. (in Chinese)

[9] OHSHIMA H, SATO K, WATANABE N. Structural analysis of suspension bridges [J]. Journal of Engineering Mechanics, 1984, 110(3): 392-404.

[10] XU X G. Key technology for erecting steel box girders of hybrid girder cable-stayed bridge over Xijiang River [J]. Railway Construction Technology, 2021 (7): 93-96. (in Chinese)

[11] ZANG Y, DAI J G, SHAO C Y. Key design techniques for Egongyan Railway Transit Bridge [J]. Bridge Construction, 2020, 50(4): 82-87. (in Chinese)

[12] YAO Q T, PAN G L, YOU X P, et al. Study on overall lifting program for steel box girder of large span of three-span continuous suspension bridge [J]. Engineering Sciences, 2013, 15(8): 54-59.

[13] DI J, ZENG K, TU X, et al. Model test study of main cable anchorage zone of Egongyan Rail Transit Special Use Bridge [J]. Bridge Construction, 2018, 48 (6): 58-63. (in Chinese)

[14] KUSANO I, BALDOMIR A, JURADO J Á, et al. The importance of correlation among flutter derivatives for the reliability based optimum design of suspension bridges [J]. Engineering Structures, 2018, 173: 416-428.

[15] KROON I B, POLK H, FUGLSANG K. 1915 Çanakkale bridge-meeting the challenge [M]//Springer Tracts on Transportation and Traffic. Cham: Springer International Publishing, 2021: 55-69.

[16] DONG M, CUI B, WANG X J. Research of three-span continuous elastic supporting suspension bridge structure system design [J]. Engineering Sciences, 2013, 15(8): 18-25. (in Chinese)

[17] QI Z C, TANG M L, CUI B, et al. The curve adjustment method of girder segments without hangers for suspension bridge with three-span continuous stiffening girder [J]. Engineering Sciences, 2013, 15(8): 37-41. (in Chinese)

[18] WANG R G. Design innovation of south channel bridge of Zhangjinggao Yangtze River Bridge [J]. Journal of Southeast University (Natural Science Edition), 2023, 53(6): 979-987. (in Chinese)

[19] ZHANG H S, ZHAO Y, RUAN J, et al. Experiment study on temperature field and effect on steel-concrete composite bridge towers [J]. Structures, 2023, 50: 937-953.

[20] YUAN Z J, WANG H, MAO J X, et al. Influence of displacement limiting cable on static and dynamic characteristics of three-span continuous suspension bridge [J]. Journal of Southeast University (Natural Science Edition), 2023, 53(3): 395-401. (in Chinese)

[21] WU J. Influence of limit sling on forces of double-tower and double-span suspension bridges [J]. Guangdong Highway Communications, 2021, 47(4): 140-143. (in Chinese)

[22] MAO J X, KE X D, SU X, et al. Fatigue performance analysis of suspenders of a long span suspension bridge under monitored traffic flow [J]. Journal of Southeast University (Natural Science Edition), 2024, 54 (4): 952-960. (in Chinese)

[23] YANG Y F, BAI W X, WEI J D. Precision analysis of dynamic characteristics of cable using Ernst's modified formula in cable-stayed bridge [J]. World Earthquake Engineering, 2008, 24(2): 50-53. (in Chinese)

[24] HUI Y, XU L. Parametric analysis of the nonlinear primary resonance of spatial cable suspension bridges [J]. Journal of Southeast University (English Edition), 2024, 40(2): 165-175.

[25] ZHU L, MENG B W, HUO X J, et al. Cable force optimization of cable-stayed bridges based on the influence matrix and elite genetic algorithm [J]. Journal of Southeast University (English Edition), 2024, 40(2): 129-139.

[26] BARKER R M, PUCKETT J A. Design of highway bridges: An LRFD approach [M]. New York: John Wiley & Sons, 2021: 485-490.

[27] WANG H, LI A Q. Influence of central buckle on wind-induced buffeting response of long-span suspension bridge [J]. China Civil Engineering Journal, 2009, 42 (7): 78-84. (in Chinese)

[28] BATHE K J, RAMASWAMY S. An accelerated subspace iteration method [J]. Computer Methods in Applied Mechanics and Engineering, 1980, 23(3): 313-331.

[29] LI A Q, ZHANG C, DENG Y, et al. Automatic identification method for structural modal parameters based on stochastic subspace identification[J]. Journal of Southeast University (Natural Science Edition), 2023, 53(1): 53-60. (in Chinese)

[30] TAO T Y, GAO W J, JIANG Z X, et al. Analysis on wind-induced vibration and its influential factors of long suspenders in the wake of bridge tower[J]. Journal of Southeast University (Natural Science Edition), 2023, 53(6): 1065-1071. (in Chinese)

大跨悬索桥主缆限位装置形式对结构力学性能的影响研究

袁智杰[1,2], 王浩[1], 茅建校[1], 李柔[1], 宗海[3]

(1. 东南大学混凝土及预应力混凝土结构教育部重点实验室, 南京 211189; 2. Laboratorio di Meccanica della Frattura, Politecnico di Torino, Torino 10129, Italy; 3. 南京公路发展(集团)有限公司, 南京 210031)

摘要: 主缆限位装置是协调连续体系悬索桥边跨主缆与主梁竖向变形的关键构件。为揭示限位装置对桥梁结构的力学作用机理,以某三跨连续悬索桥为工程背景,通过数值模拟探究了不同形式的限位装置对大桥边跨区域主缆线形、主梁线形、构件内力及结构动力特性的影响。研究结果表明,不设限位装置时,边跨处的主缆与主梁将产生较大的竖向位移,同时引起其余吊索发生应力重分布,极大降低了边跨处吊索的安全系数。设置限位装置在一定程度上可以提高结构的竖向刚度。刚性限位装置自身内力较大,但对于边跨主梁内力的整体控制效果稍好于柔性限位装置。不同形式的限位装置均可有效协调边跨区域缆梁变形及应力的分布。限位装置的形式取决于桥址区地形因素及边跨相关构件的设计要求。

关键词: 大跨悬索桥;限位装置;静动力特性;有限元;活载

中图分类号: U448.27